Mechanochromic Materials

Deutsche Ausgabe: DOI: 10.1002/ange.201602602
Internationale Ausgabe: DOI: 10.1002/anie.201602602

Bismuth-Based Coordination Polymers with Efficient Aggregation-Induced Phosphorescence and Reversible Mechanochromic Luminescence

Oksana Toma, Magali Allain, Francesco Meinardi, Alessandra Forni, Chiara Botta,* and Nicolas Mercier**

Abstract: *Two bismuth coordination polymers (CPs), (TBA)-[$BiBr_4$(bp4mo)] (TBA = tetrabutylammonium) and [$BiBr_3$-(bp4mo)$_2$], which are based on the rarely used simple ditopic ligand N-oxide-4,4′-bipyridine (bp4mo), show mechanochromic luminescence (MCL). High solid-state phosphorescence quantum yields of up to 85 % were determined for (TBA)-[$BiBr_4$(bp4mo)] (λ_{em} = 540 nm). Thorough investigations of the luminescence properties combined with DFT and TDDFT calculations revealed that the emission is due to aggregation-induced phosphorescence (AIP). Upon grinding, both samples became amorphous, and their luminescence changed from yellow to orange and red, respectively. Heating or exposure to water vapor led to the recovery of the initial luminescence. These materials are the first examples of mechanochromic phosphors based on bismuth(III).*

The search for solid-state luminescent materials and materials with tunable luminescence, such as those exhibiting mechanochromic luminescence (MCL), is of great interest owing to their enormous potential in optical and optoelectronic devices, such as lighting and displays, memory devices, and sensors. The use of luminogens based on various complexes and coordination polymers (CPs) is very promising in fields such as lighting technology[1] or chemical sensors (porous CPs).[2] A disadvantage of molecular luminogens, including CPs, can be the reduction of the emission efficiency upon aggregation as a result of concentration quenching (aggregation-caused quenching, ACQ). However, in some cases, the restriction of intramolecular motion (RIM) that is observed upon aggregation can also have the opposite effect, namely an increase in the emission efficiency as a result of the blocking of rotations and vibrations that are responsible for non-radiative pathways in non-rigid environments: This process is called AIE (aggregation-induced emission) or AIP (aggregation-induced phosphorescence).[3–7] Such materials have received much attention in the past decade because they have great potentialities for MCL compared to non-AIE materials.[8–17] MCL compounds are smart materials whose emission color changes when a mechanical force such as grinding is applied. Some of these materials can also recover their initial emission upon exposure to vapors or heating. Most MCL materials are AIE organic compounds[9,13] (mainly pyrene[11] and anthracene[12] derivatives) whose changes in emission are usually accompanied by the amorphization of the sample, which is due to their conformational flexibility and the facile modification of weak intermolecular interactions (π–π, weak hydrogen bonding) under pressure. Metal complexes are another interesting class of materials that may exhibit MCL.[8] Most of these complexes are based on Pt^{II}[14] and Ir^{III},[15] whereas some based on Au^{I}, Zn^{II}, Ag^{I}, Cu^{I}, and Al^{III} have also been reported.[8,16,17]

In contrast to the well-known, commercially available ditopic ligand *N*,*N*′-dioxide-4,4′-bipyridine (bp4do), which is extensively used in the CP field,[18] *N*-oxide-4,4′-bipyridine (bp4mo) has rarely been used.[19] To the best of our knowledge, no bismuth complexes or CPs based on bp4mo or bp4do have been reported thus far, whereas we recently showed the ability of bipyridinium derivatives, including one pyridyl-*N*-oxide and *N*-oxide-2,2′-bipyridine, to bind bismuth ions, giving AIE complexes.[20] Moreover, bismuth ions and halides have a great tendency to form halobismuthate anions, particularly with bipyridinium derivatives.[21] Herein, we report two luminescent CP materials obtained with the $BiBr_3$/bp4mo system: (TBA)[$BiBr_4$(bp4mo)] (**1**; TBA = tetrabutylammonium) and [$BiBr_3$(bp4mo)$_2$] (**2**) show AIP with quantum yields (QYs) of 85 % (**1**) and 15 % (**2**). Furthermore, both materials exhibit MCL, which is unprecedented for bismuth(III)-based compounds.

CP **1** was obtained as yellow needle-like crystals by the slow evaporation of a mixture of bp4mo·2H_2O, $BiBr_3$, and (TBA)Br, whereas yellow crystals of **2** were prepared by a solvothermal method from a mixture of $BiBr_3$, bp4mo·2H_2O, and (TBA)Br in MeCN at 75 °C. The asymmetric unit of the structure of **1** includes one bp4mo molecule

[*] Dr. O. Toma, M. Allain, Prof. N. Mercier
MOLTECH-Anjou, UMR-CNRS 6200, University of Angers
2 Bd Lavoisier, 49045 Angers (France)
E-mail: nicolas.mercier@univ-angers.fr
Dr. C. Botta
Istituto per lo Studio delle Macromolecole (ISMAC), CNR
Via Corti 12, 20133 Milano (Italy)
E-mail: c.botta@ismac.cnr.it
Dr. A. Forni
Istituto di Scienze e Tecnologie Molecolari
Università degli Studi di Milano
via C. Golgi 19, 20133 Milano (Italy)
E-mail: a.forni@istm.cnr.it
Dr. F. Meinardi
Dipartimento di Scienza dei Materiali
Università degli Studi di Milano Bicocca
via Cozzi 55, 20125 Milano (Italy)
Supporting information and the ORCID identification numbers for the authors of this article can be found under http://dx.doi.org/10.1002/anie.201602602.

and two bismuth ions located on symmetry centers.[22] They form a one-dimensional (1D) coordination polymer with bp4mo molecules bridging the Bi(1) and Bi(2) ions. As already seen in a lead compound based on 2D networks,[19a] while one Bi^{III} ion is *trans*-connected to two pyridyl N atoms, the other one is *trans*-connected to two pyridyl-*N*-oxide O atoms; each Bi^{III} ion is also surrounded by four terminal bromides, leading to $Bi(1)O_2Br_4$ and $Bi(2)N_2Br_4$ pseudo-octahedra. The N-O-Bi bond angle is close to 120° (124.2°), as usually observed for the coordination of pyridine-*N*-oxide rings, while the dihedral angle between the two pyridyl rings of bp4mo is 21°. The 1D networks are displaced from each other in such a way that there are lateral CH···Br contacts between bromide and bp4mo, which define the 2D supramolecular network (Figure 1 a). The anionic networks $[BiBr_4(bp4mo)]^-$ are counterbalanced by the TBA^+ cations. These bulky entities are located in between two 2D consecutive supramolecular assemblies as showed in Figure 1 b. It is noteworthy that there are no close face contacts between bp4mo molecules in the structure of **1**.

The asymmetric unit of the structure of $[BiBr_3(bp4mo)_2]$ (**2**) contains one bismuth ion and two bp4mo molecules.[22] Both components define neutral 1D coordination polymers. The two kinds of bp4mo molecules have very different roles. As in the structure of **1**, one connects two bismuth ions, which leads to a *cis*-connected 1D network along the *b* direction, while the other one is linked to only one bismuth ion via the pyridyl-*N*-oxide moiety (Figure 1 c). The Bi^{III} ion, which is surrounded by three bromides, one N, and two O atoms belonging to bp4mo molecules, is roughly found in the plane of the pyridyl moiety to which it is connected, while it is out of the plane of the connecting pyridyl-*N*-oxide moieties, with N-O-Bi bond angles again close to 120° (115.8° and 119.8° for bridging and terminal bp4mo, respectively). The dihedral angles between two pyridyl rings are 24° and 18° for bridging bp4mo and terminal bp4mo, respectively. The 1D networks are interlaced, thus forming a densely packed structure (Figure 1 c).

The absorption and emission spectra of CPs **1** and **2** are shown in Figure 2. In the solid state, the lowest-energy absorption band has a maximum at approximately $\lambda_{abs,max} =$ 415 nm for **1** and 410 nm for **2**. In CH_2Cl_2, the first absorption band of both **1** and **2** is located at $\lambda_{abs,max} = 390$ nm, and thus significantly red-shifted with respect to the corresponding absorption band of the ligand ($\lambda_{abs,max} = 312$ nm).

Time-dependent density functional theory (TDDFT) calculations in CH_2Cl_2 on the oligomeric model compounds **1″** and **2″**, which simulate the infinite chains of **1** and **2** (see the Supporting Information for computational details), gave lowest excitation energies of $\lambda_{abs,max} = 409$ nm (oscillator strength $f = 0.56$) and 352 nm ($f = 0.47$), respectively. Upon looking at the involved orbitals (Figure 3; see also the Supporting Information, Figures S3–S5 and Table S1), the CT character of the transitions from the inorganic moiety of the complexes (Bi and Br) to the organic ligand becomes evident. In the case of **2**, both kinds of bp4mo molecules (bridging and terminal) play an important role. These low-energy transitions closely resemble, both in nature and energy, that previously reported for the related $[BiBr_3(bp2mo)_2]$ (bp2mo = *N*-oxide-2,2′-bipyridine) complex.[20c] The absorption bands observed at about $\lambda_{abs,max} = 310$ nm for both **1** and **2** in solution were also reproduced by our calculations, which provided a series of transitions with maxima at $\lambda_{abs,max} = 290$ nm for both **1″** and **2″**, which were assigned to intraligand charge transfer. Finally, the transitions below 290 nm involve orbitals localized on the ligands or bromine atoms.

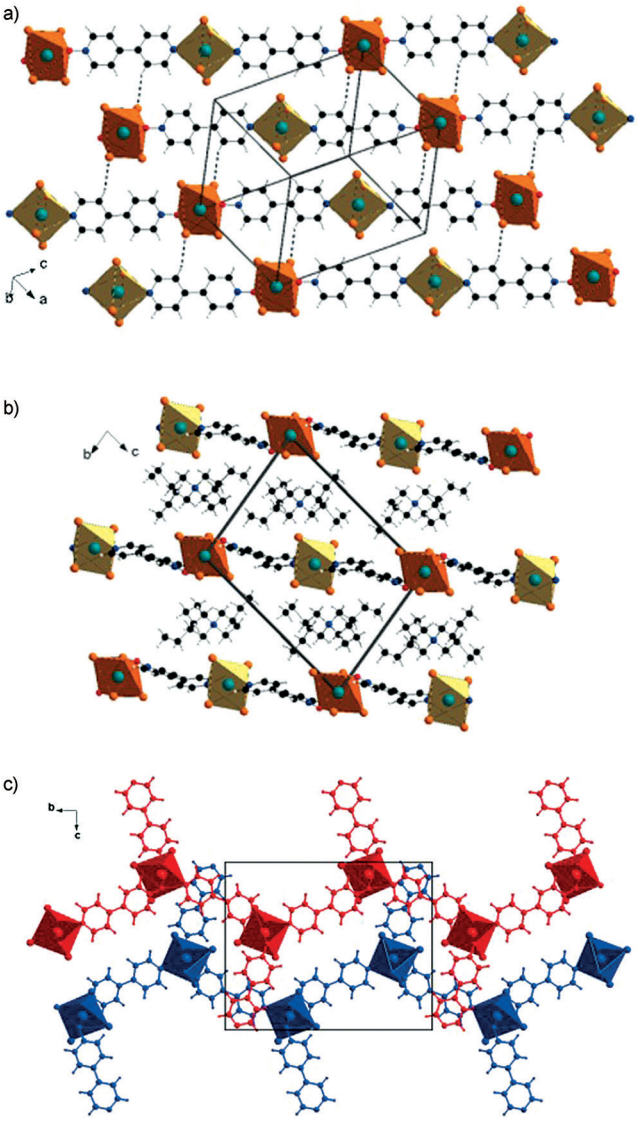

Figure 1. General views of **1** showing a) adjacent 1D networks (H···Br interactions of < 3.0 Å are represented by dashed lines) and b) the TBA^+ cations separating the 2D layers. c) General view of **2** showing two adjacent 1D CPs.

As observed for the previously reported AIP complex $[BiBr_3(bp2mo)_2]$,[20c] photoluminescence was hardly detectable in solution (PL QYs below 0.1 % for both **1** and **2**), whereas powders of **1** and **2** showed bright yellow-orange emission (Figure 2 b). The PL efficiencies of the powders were determined to be 85 % and 11 % for **1** and **2**, respectively, with lifetimes of 18 and 1 μs (Table S2). Interestingly, the lifetime of the weak blue emission in solution is very short (ca. 10 ps),

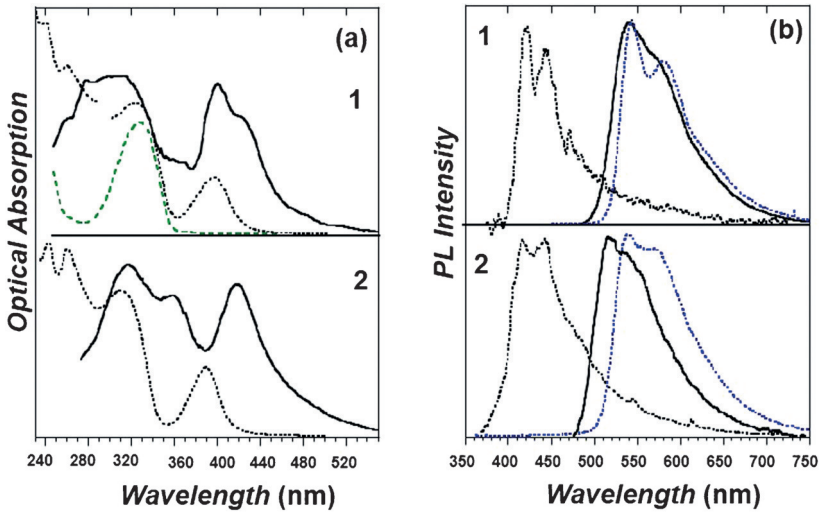

Figure 2. a) Absorption and b) PL spectra of **1** and **2** in the solid state (solid line) and in solution (dotted line) at room temperature (black) and 100 K (blue). Absorption spectrum of bp4mo (dashed green line) in solution.

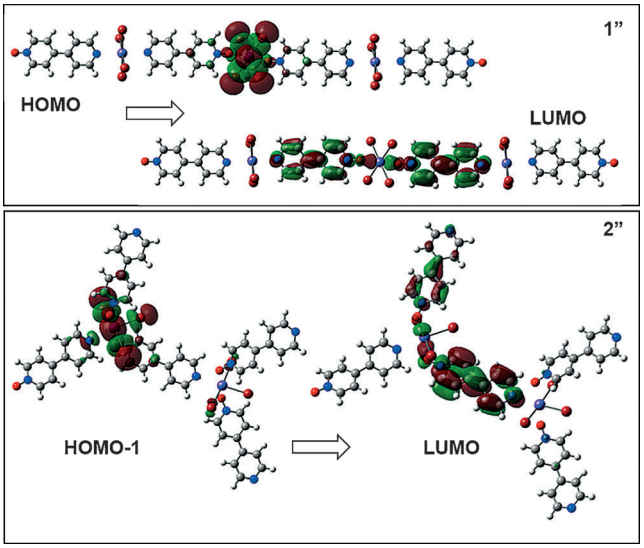

Figure 3. The main M062X/def2-SVP molecular orbitals involved in the lowest-energy transitions of **1″** (top) and **2″** (bottom; isosurface values: 0.02).

suggesting that the emissive state is of a different nature and that a very efficient deactivation pathway for the complexes is operating in solution (Figure S7). When the intramolecular motions were frozen upon lowering the temperature below the solidification point of the solvent (Figures S8 and S9), the solution showed bright yellow emission with a red-shifted PL spectrum that resembled the solid-state one (see Figure 2b). The different nature of the emissive states (triplets) in rigid environments (solid state and frozen solution) and solution (singlet) suggests that the presence of a heavy atom such as Bi enables the fast decay of S_1 states by intersystem crossing to the low-lying T_1 state, whose long-lived phosphorescence is completely quenched in solution by free intramolecular motions. In contrast, the short-lived singlet state still shows weak blue fluorescence in non-rigid environments. The remarkable differences in the PL quantum yields of **1** and **2** in the solid state might be related to the presence of non-emissive traps in the latter, which was confirmed by time-resolved analysis of the PL at different temperatures (see Figure S10).

Both compounds **1** and **2** exhibit mechanochromic luminescence. Upon grinding a sample in a mortar for a few minutes, the luminescence changed from yellow ($\lambda =$ 540 nm, **1**) to orange ($\lambda = 585$ nm, **1-g**, where -g corresponds to grinded material) and from greenish-yellow ($\lambda = 516$ nm, **2**) to orange-red ($\lambda = 622$ nm, **2-g**; Figure 4a,b) while the colors of the samples remained unchanged. The wavelength shift of $\Delta\lambda =$ 106 nm for **2** is one of the largest ever reported for MCL complexes.[8] As often observed, the samples became amorphous upon grinding, which was revealed by the absence of XRPD lines for **1-g** (Figure 4c), whereas the lines became broader for **2-g** (Figure S13). Thermal analysis by differential scanning calorimetry (DSC) of **1-g** revealed a strong exothermic process at 80 °C, which was assigned to a crystallization process, as confirmed by the appearance of XRPD lines (**1-g,Δ**; Δ = heated; Figure 4c). In contrast, such an exothermic peak was not observed for **2-g**. Therefore, the overall process can be rendered reversible by heating **1-g** (Figure S12), whereas heating **2-g** had no effect.

However, reversible emission changes were clearly seen by the naked eye for both **1-g** and **2-g** when samples were exposed to a saturated water atmosphere for a few hours (**1-g,H_2O** and **2-g,H_2O**). Nevertheless, the reversibility was only partial for **2-g**, as shown by PL measurements (Figure S12). Compounds **1-g** and **2-g** are stable for at least two months at room temperature, and samples thereof can be grinded/heated several times (for **1**/**1-g**) without any changes to the switch in emission. As for most MCL materials that exhibit a crystal-to-amorphous transition, the origin of the MCL in **1** and **2** can be tentatively assigned to a change in the crystal packing involving a different pattern of weak interactions such as hydrogen bonding (**1**, **2**) or π–π interactions (**2**). We also suggest that the pyridine NO–Bi bond is a key parameter. In fact, while keeping the N-O-Bi bond angle close to 120°, the O–Bi bond could rotate with respect to the N–O bond, leading to a conformational change that could involve a rearrangement of the emitting electronic levels without suppression of the RIM properties of the material. Further work will focus on this aspect.

In conclusion, we have reported two coordination polymers based on bismuth(III) and the simple ditopic ligand *N*-oxide-4,4′-bipyridine (bp4mo). (TBA)[$BiBr_4$(bp4mo)] and [$BiBr_3$(bp4mo)$_2$] exhibit aggregation-induced phosphorescence with high quantum yields of up to 85%. These are the first bismuth-containing compounds that exhibit mechanochromic luminescence, and this process is fully reversible upon heating in the case of **1**. The clear change in the emission color observed for both compounds upon grinding and H_2O

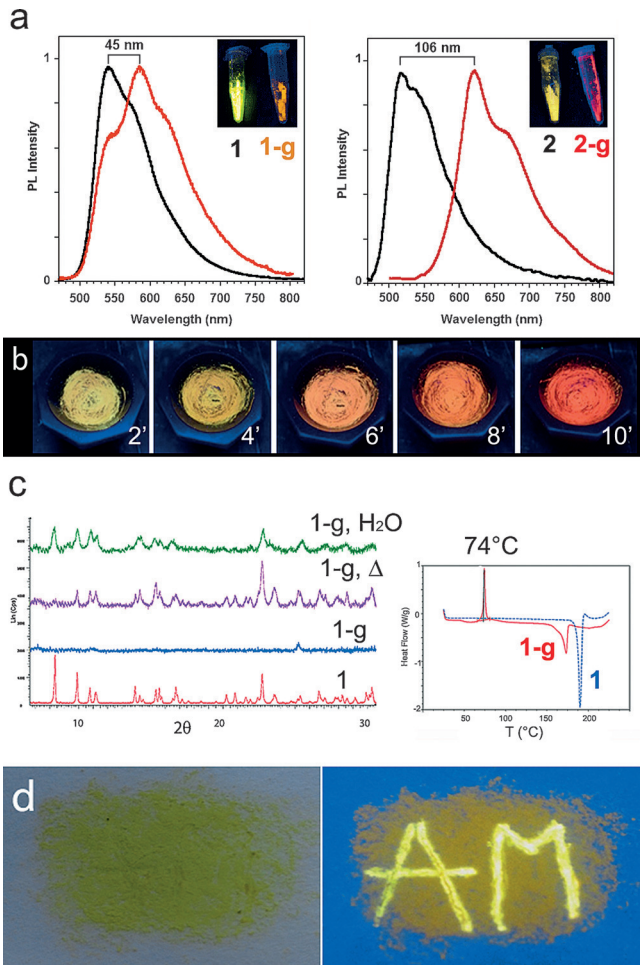

Figure 4. MCL properties of **1** and **2**. a) PL spectra of **1** and **1-g** (left) and **2** and **2-g** (right). Inset: photographs under UV light. b) Grinding of **2** in a mortar, photographs under UV light. c) XRPD patterns of **1**, **1-g**, **1-g,Δ**, and **1-g,H_2O** (left) and DSC curves (right) of **1** and **1-g**. d) Photographs under ambient light (left) and UV light (right) of letters written on a **1-g** sample with a heating pen.

vapor exposure makes them ideal candidates for humidity sensors. A key parameter of the change in luminescence could be the conformational change of the NO–Bi moiety. We anticipate that **1** and **2** are the first compounds of a new family of MCL materials.

Acknowledgements

A.F. thanks the MIUR for supporting the PRIN 2010–2011 project (2010ERFKXL). N.M. thanks the LUMOMAT regional program for a postdoctoral fellowship to O.T. (Bipylum project).

Keywords: bismuth · coordination polymers · luminescence · mechanochromic materials · N,O ligands

How to cite: *Angew. Chem. Int. Ed.* **2016**, *55*, 7998–8002
Angew. Chem. **2016**, *128*, 8130–8134

[1] a) Y. Cui, Y. Yue, G. Qian, B. Chen, *Chem. Rev.* **2012**, *112*, 1126–1162; b) J. Heine, K. Müller-Buschbaum, *Chem. Soc. Rev.* **2013**, *42*, 9232–9242; c) H. Xu, J. Wang, Y. Wei, G. Xie, Q. Xue, Z. Denga, W. Huang, *J. Mater. Chem. C* **2015**, *3*, 1893–1903; d) E. Cariati, E. Lucenti, C. Botta, U. Giovanella, D. Marinotto, S. Righetto, *Coord. Chem. Rev.* **2016**, *306*, 566–614.

[2] a) L. E. Kreno, K. Leong, O. K. Farha, M. Allendorf, R. P. Van Duyne, J. T. Hupp, *Chem. Rev.* **2012**, *112*, 1105–1125; b) Y. Takashima, V. M. Martinez, S. Furukawa, M. Kondo, S. Shimomura, H. Uehara, M. Nakahama, K. Sigimoto, S. Kitagawa, *Nat. Commun.* **2011**, *2*, 168–175; c) Z. Hu, B. J. Deibert, J. Li, *Chem. Soc. Rev.* **2014**, *43*, 5815–5840; d) D. Liu, K. Lu, C. Poon, W. Lin, *Inorg. Chem.* **2014**, *53*, 1916–1924; e) K. Müller-Buschbaum, F. Beuerle, C. Feldmann, *Microporous Mesoporous Mater.* **2015**, *216*, 171–199.

[3] J. W. Y. Lam, B. Z. Tang, *Chem. Soc. Rev.* **2011**, *40*, 5361–5388.

[4] a) Q. Zhao, L. Li, F. Y. Li, M. X. Yu, Z. P. Liu, T. Yi, C. H. Huang, *Chem. Commun.* **2008**, 685–687; b) K. W. Huang, H. Z. Wu, M. Shi, F. Y. Li, T. Yi, C. H. Huang, *Chem. Commun.* **2009**, 1243–1245; c) E. Cariati, V. Lanzeni, E. Tordin, R. Ugo, C. Botta, A. Giacometti Schieroni, A. Sironi, D. Pasini, *Phys. Chem. Chem. Phys.* **2011**, *13*, 18005–18014.

[5] a) J. Mei, Y. Hong, J. W. Y. Lam, A. Qin, Y. Tang, B. Z. Tang, *Adv. Mater.* **2014**, *26*, 5429–5479; b) J. Mei, N. L. C. Leung, R. T. K. Kwok, J. W. Y. Lam, B. Z. Tang, *Chem. Rev.* **2015**, *115*, 11718–11940.

[6] a) G. Li, Y. Wu, G. Shan, W. Che, D. Zhu, B. Song, L. Yan, Z. Su, M. R. Bryce, *Chem. Commun.* **2014**, *50*, 6977–6980; b) J. Wang, J. Mei, R. Hu, J. Z. Sun, A. Qin, B. Z. Tang, *J. Am. Chem. Soc.* **2012**, *134*, 9956–9966.

[7] a) N. B. Shustova, T.-C. Ong, A. F. Cozzolino, V. K. Michaelis, R. G. Griffin, M. Dinc, *J. Am. Chem. Soc.* **2012**, *134*, 15061–15070; b) E. Quartapelle Procopio, M. Mauro, M. Panigati, D. Donghi, P. Mercandelli, A. Sironi, G. D'Alfonso, L. De Cola, *J. Am. Chem. Soc.* **2010**, *132*, 14397–14399; c) S. Liu, H. Sun, Y. Ma, S. Ye, X. Liu, X. Zhou, X. Mou, L. Wang, Q. Zhao, W. J. Huang, *Mater. Chem.* **2012**, *22*, 22167–22173.

[8] X. Zhang, Z. Chi, Y. Zhang, S. Liu, J. Xu, *J. Mater. Chem. C* **2013**, *1*, 3376–3390.

[9] a) Y. Q. Dong, J. W. Y. Lam, B. Z. Tang, *J. Phys. Chem. Lett.* **2015**, *6*, 3429–3436; b) C. Botta, S. Benedini, L. Carlucci, A. Forni, D. Marinotto, A. Nitti, D. Pasini, S. Righetto, E. Cariati, *J. Mater. Chem. C* **2016**, *4*, 2979–2989.

[10] Y. Sagara, T. Kato, *Nat. Chem.* **2009**, *1*, 605–610.

[11] a) Y. Sagara, T. Mutai, I. Yoshikawa, K. Araki, *J. Am. Chem. Soc.* **2007**, *129*, 1520–1521; b) Y. Sagara, T. Komatsu, T. Ueno, K. Hanaoka, T. Kato, T. Nagano, *Adv. Funct. Mater.* **2013**, *23*, 5277–5284.

[12] a) Y. Dong, B. Xu, J. Zhang, X. Tan, L. Wang, J. Chen, H. Lv, S. Wen, B. Li, L. Ye, B. Zou, W. Tian, *Angew. Chem. Int. Ed.* **2012**, *51*, 10782–10785; *Angew. Chem.* **2012**, *124*, 10940–10943; b) L. Bu, M. Sun, D. Zhang, W. Liu, Y. Wang, M. Zheng, S. Xue, W. Yang, *J. Mater. Chem. C* **2013**, *1*, 2028–2035.

[13] Z. Chi, X. Zhang, B. Xi, X. Zhou, C. Ma, Y. Zhang, S. Liu, J. Xu, *Chem. Soc. Rev.* **2012**, *41*, 3878–3896.

[14] X.-P. Zhang, J.-F. Mei, J.-C. Lai, C.-H. Li, X.-Z. You, *J. Mater. Chem. C* **2015**, *3*, 2350–2357.

[15] H. Sun, S. Liu, W. Lin, K. Y. Zhang, W. Lv, X. Huang, F. Huo, H. Yang, G. Jenkins, Q. Zhao, W. Huang, *Nat. Commun.* **2014**, *5*, 3601–3609.

[16] S. Perruchas, X. F. Le Goff, S. Maron, I. Maurin, F. Guillen, A. Garcia, T. Gacoin, J. P. Boilot, *J. Am. Chem. Soc.* **2010**, *132*, 10967–10969.

[17] P. Baranyai, G. Marsi, C. Jobbagy, A. Domjan, L. Olah, A. Deak, *Dalton Trans.* **2015**, *44*, 13455–13459.

[18] a) A.-C. Chamayou, C. Janiak, *Inorg. Chim. Acta* **2010**, *363*, 2193 – 2200; b) J. Jia, A. J. Blake, N. R. Champness, P. Hubberstey, C. Wilson, M. Schröder, *Inorg. Chem.* **2008**, *47*, 8652 – 8664; c) H. W. Roesky, M. Andruh, *Coord. Chem. Rev.* **2003**, *236*, 91 – 119; d) R. J. Hill, D.-L. Long, N. R. Champness, P. Hubberstey, M. Schröder, *Acc. Chem. Res.* **2005**, *38*, 335 – 348.

[19] a) O. Toma, N. Mercier, M. Bouilland, M. Allain, *CrystEngComm* **2012**, *14*, 7844 – 7847; b) D. J. Hoffart, N. C. Habermehl, S. J. Loeb, *Dalton Trans.* **2007**, 2870 – 2875.

[20] a) O. Toma, N. Mercier, C. Botta, *Eur. J. Inorg. Chem.* **2013**, 1113 – 1117; b) O. Toma, N. Mercier, M. Allain, C. Botta, *CrystEngComm* **2013**, *15*, 8565 – 8571; c) O. Toma, N. Mercier, M. Allain, A. Forni, F. Meinardi, C. Botta, *Dalton Trans.* **2015**, *44*, 14589 – 14593.

[21] a) R.-G. Lin, G. Xu, G. Lu, M.-S. Wang, P.-X. Li, G.-C. Guo, *Inorg. Chem.* **2014**, *53*, 5538 – 5545; b) R.-G. Lin, G. Xu, M.-S. Wang, G. Lu, P.-X. Li, G.-C. Guo, *Inorg. Chem.* **2013**, *52*, 1199 – 1205; c) G. Xu, G. Guo, M. Wang, Z. Zhang, W. Chen, J. Huang, *Angew. Chem. Int. Ed.* **2007**, *46*, 3249 – 3251; *Angew. Chem.* **2007**, *119*, 3313 – 3315; d) G. Xu, G.-C. Guo, J.-S. Guo, S.-P. Guo, X.-M. Jiang, C. Yang, M.-S. Wang, Z.-J. Zhang, *Dalton Trans.* **2010**, *39*, 8688 – 8692; e) N. Mercier, *Eur. J. Inorg. Chem.* **2013**, 19 – 31.

[22] Crystal data for **1**: $C_{26}H_{44}BiBr_4N_3O$; $M = 943.26$; triclinic, $P\bar{1}$; $a = 8.7494(4)$, $b = 13.0571(6)$, $c = 16.442(1)$ Å, $\alpha = 76.81(1)$, $\beta = 77.15(1)$, $\gamma = 72.40(1)°$, $V = 1719.28(2)$ Å^3; $Z = 2$; $T = 293(2)$ K; $\mu(\text{Mo}) = 9.80$ mm^{-1}; $2\theta_{max} = 28.03°$; 8252 unique reflections (R(int) = 0.050); 319 parameters; $R1(I < 2\sigma(I)) = 0.037$; $wR2$ (all data) = 0.079. Crystal data for **2**: $C_{20}H_{16}BiBr_3N_4O_2$; $M = 793.08$; monoclinic, $P21/c$; $a = 7.1074(4)$, $b = 19.7546(16)$, $c = 16.1960(15)$ Å, $\beta = 94.22(1)°$, $V = 2267.8(3)$ Å^3; $Z = 4$; $T = 293(2)$ K; $\mu(\text{Mo}) = 13.08$ mm^{-1}; $2\theta_{max} = 30.01°$; 6449 unique reflections (R(int) = 0.057); 271 parameters; $R1(I < 2\sigma(I)) = 0.035$; $wR2$ (all data) = 0.067. X-ray diffraction data were collected on a Bruker-Nonius KAPPA-CDD diffractometer with graphite-monochromated MoKα radiation ($\lambda = 0.71073$ Å). Structures were solved and refined using the Shelxl97 package. Positions and atomic displacement parameters were refined by full-matrix least-squares routines against F^2. All hydrogen atoms were treated with a riding model. CCDC 1415242 (**1**) and 1415244 (**2**) contain the supplementary crystallographic data for this paper. These data are provided free of charge by The Cambridge Crystallographic Data Centre.

Received: March 14, 2016
Published online: May 11, 2016

